British Journal of Cancer www.nature.com/bjc

ARTICLE

Translational Therapeutics

Andrographolide sensitizes glioma to temozolomide by inhibiting DKK1 expression

Zhan-Sheng Zhang[1,2,4], Zi-Xuan Gao[1,2,4], Jin-Jin He[1,4], Can Ma[2], Hang-Tian Tao[2], Feng-Yi Zhu[2], Yu-Na Cheng[2], Cui-Qing Xie[2], Ji-Qin Li[2], Zhuang-Zhuang Liu[2], Li-Li Hou[2], Hua Sun[2]✉, Song-Qiang Xie[1,2,3]✉ and Dong Fang[1,2,3]✉

BACKGROUND: Temozolomide (TMZ) is the first-line chemotherapeutic drug for gliomas treatment. However, the clinical efficacy of TMZ in glioma patients was very limited. Therefore, it is urgently needed to discover a novel approach to increase the sensitivity of glioma cells to TMZ.

METHODS: Western blot, immunohistochemical staining, and qRT-PCR assays were used to explore the mechanisms underlying TMZ promoting DKK1 expression and andrographolide (AND) inhibiting DKK1 expression. HPLC was used to detect the ability of andrographolide (AND) to penetrate the blood-brain barrier. MTT assay, bioluminescence images, magnetic resonance imaging (MRI) and H&E staining were employed to measure the proliferative activity of glioma cells and the growth of intracranial tumors.

RESULTS: TMZ can promote DKK1 expression in glioma cells and brain tumors of an orthotopic model of glioma. DKK1 could promote glioma cell proliferation and tumor growth in an orthotopic model of glioma. Mechanistically, TMZ increased EGFR expression and subsequently induced the activation of its downstream MEK-ERK and PI3K-Akt pathways, thereby promoting DKK1 expression in glioma cells. Andrographolide inhibited TMZ-induced DKK1 expression through inactivating MEK-ERK and PI3K-Akt pathways. Andrographolide can cross the blood-brain barrier, the combination of TMZ and andrographolide not only improved the anti-tumor effects of TMZ but also showed a survival benefit in an orthotopic model of glioma.

CONCLUSION: Andrographolide can enhance anti-tumor activity of TMZ against glioma by inhibiting DKK1 expression.

British Journal of Cancer; https://doi.org/10.1038/s41416-024-02842-0

BACKGROUND

Glioma is the most common primary malignant brain tumor, which is characterized by high mortality, high recurrence, and low cure rate [1]. The current treatment strategy for gliomas is neurosurgical resection followed by concomitant radiotherapy and chemotherapy [2]. Temozolomide (TMZ), a second-generation alkylating agent, is the first-line chemotherapeutic drug used in the treatment of glioma [3]. However, the clinical outcome of TMZ chemotherapy remains unsatisfactory due to the development of resistance to TMZ [4]. Therefore, it is urgently needed to discover a novel approach to increase the sensitivity of glioma cells to TMZ.

Dickkopf-1 (DKK1), a secreted glycoprotein, was originally identified as a head inducer by inhibiting Wnt/β-catenin signaling during vertebrate development [5]. Given that Wnt/β-catenin signaling plays a critical role in driving tumor occurrence, development, recurrence, and metastasis, DKK1 was therefore supposed to be a tumor suppressor [6–8]. However, DKK1 overexpression has been observed in several types of cancer, and its expression is associated with a poor prognosis of cancer patients, suggesting that DKK1 can also serve as an oncogenic protein [9–11]. It was later found that DKK1 can signal through a Wnt receptor-independent pathway to promote tumor progression [12, 13]. Notably, chemotherapeutic agents such as cisplatin and 5-fluorouracil can promote DKK1 expression at the transcriptional level, and knockdown of DKK1 sensitizes cancer cells to these agents in non-small cell lung cancer (NSCLC) and colorectal cancer (CRC) [14, 15]. However, whether DKK1 could be used as a sensitizing target for TMZ in glioma remains unknown. Therefore, this study aimed at decipher the role of DKK1 in the process of TMZ against glioma.

Natural products have been widely used in the cancer treatment as an alternative therapy due to their enhancing the antitumor effects of chemotherapy or reducing the side effects of conventional therapies [16, 17]. Andrographolide, a diterpenoid lactone isolated from the plant Andrographis paniculate, has shown versatile potency against various diseases including cancer [18, 19]. Mechanistic studies suggested that andrographolide exerts anti-tumor effects by inactivating cellular signaling

[1]Department of Pharmacy, The First Affffliated Hospital of Henan University, N. Jinming Ave, Kaifeng 475004, China. [2]Institute of Chemical Biology, School of Pharmacy, Henan University, N. Jinming Ave, Kaifeng 475004, China. [3]Henan Province Engineering Research Center of High Value Utilization to Natural Medical Resource in Yellow River Basin, Kaifeng 475004, China. [4]These authors contributed equally: Zhan-Sheng Zhang, Zi-Xuan Gao, Jin-Jin He. ✉email: sunhua@vip.henu.edu.cn; xiesq@henu.edu.cn; fangdong@henu.edu.cn

Received: 4 July 2023 Revised: 17 August 2024 Accepted: 28 August 2024
Published online: 12 September 2024

pathways related to proliferation and inducing cell cycle arrest [20, 21]. In addition to its direct anti-cancer potential, andrographolide also exerts synergistic inhibitory effects combined with chemotherapy drugs including 5-fluorouracil and cisplatin [15, 22]. Although andrographolide was reported to induce apoptosis of glioma cells in vitro [20, 23], whether it can be used to sensitize glioma to TMZ-based therapy remains to be explored. In this study, our findings suggested that andrographolide enhance anti-tumor activity of TMZ against glioma by inhibiting DKK1 expression.

METHODS

Reagents and antibodies

Temozolomide (T2577), andrographolide (365645) and AG1478 (T4182) were purchased from Sigma-Aldrich (Darmstadt, Germany). Rabbit monoclonal anti-DKK1 antibody (ab109416) and rabbit monoclonal anti-EGFR antibody (ab32077) were obtained from Abcam (Cambridge, MA, USA). Rabbit monoclonal anti-phospho-AKT (Ser 473) (#4060), rabbit monoclonal anti-Akt (#4685), rabbit monoclonal anti-p44/42 MAPK (#4695), and rabbit monoclonal anti-p-p42/44 MAPK (Thr202/Tyr204) (#4370) were purchased from Cell Signaling Technology (Danvers, MA, USA).

Cell lines and cell culture

Human glioma cell lines (U87, U251, U-118MG and A172 cells) and mouse glioma 261 (Gl261) cells were obtained from Cell Bank of the Chinese Academy of Science (Shanghai, China). Cells were cultured in Dulbecco's modified Eagle's medium (Gibco, Carlsbad, CA) containing 10% fetal bovine serum (Gibco), penicillin (100 units/mL) and streptomycin (100 units/mL) at 37°C in humidified incubator containing 5% CO_2.

Plasmid construction and lentivirus production

The lentivirus vectors expressing DKK1 were constructed by inserting the DKK1 cDNA into pCDH-CMV-MCS-EF1-CopGFP-T2A-Puro. To construct the lentivirus vectors harboring DKK1 shRNA, an oligo DNA fragment containing DKK1 shRNA were cloned into hU6-MCS-CBh-gcGFP-IRES-puromycin. The lentivirus particles were constructed by transfecting 293 T cells with envelope plasmid pMD2.G and packaging plasmid psPAX2. The lentivirus productions were collected and filtered using 0.45 μm filters at 24 h and 48 h after transfection, Next, the lentivirus productions were used to treat cells in culture. After 48 h of transfection, the cells were selected in the presence of 1.5 μg/ml puromycin (Sigma, St. Louis, USA). For short-term overexpression of EGFR, the plasmids pEGFP-N1-EGFR(EGFR-OE) and vector were transfected into glioma cells using Lipofectamine 2000 DNA Transfection Reagent (Invitrogen, Carlsbad, CA, USA) according to the manufacturer's instruction.

Cell viability assay

Cell viability was determined by 3-(4, 5-dimethyl-2-thiazolyl)-2,5-diphenyl-2-H-tetrazolium bromide (MTT) assay. Glioma cells (1000 per well) were seeded in 96-well plates. Cell viability was measured at 0 d, 1 d, 2 d, 3 d, 4 d and 5 d after plating. 10 μL of MTT solution (5 mg/mL) was added to each well and the plates were maintained at 37°C for another 4 h. The formed formazan crystals in each well were dissolved in 100 μL DMSO. The absorbance values were measured at 570 nm using a microplate reader (Thermo Scientific, Rockford, IL), quantification was assessed based on the optical density values.

Real-time PCR

Total RNA from glioma cells was extracted using TRIzol reagent (Invitrogen, CA, USA). Complementary DNA was synthesized using the Takara PrimeScript TM RT Master Mix Kit (Takara, Tokyo, Japan) according to the manufacturer's instructions. Real-time PCR was performed using 2× SYBR Green PCR Master Mix (Promega) on an ABI 7500 sequence detection system (Applied Biosystems). The reaction conditions were as follows: 95 °C, predenaturation for 5 min, 15 s at 95°C, and 1 min at 60°C for a total of 40 cycles. Glyceraldehyde-3-phosphate dehydrogenase (GAPDH) was used as an internal control. The relative expression level of the genes was calculated by the $2^{-\Delta\Delta Ct}$ method. Specific primers for human glioma cells were as follows: DKK1, 5′- CCA CTT TGA TCT CAC GCGTC-3′ (Forward) and 5′- AGA GAG GGA GGC GAG AGACT-3′ (Reverse); GAPDH, 5′-GAC ACC CAC TCC TCC ACC TTT-3′ (Forward) and 5′-TTG CTG TAG CCA AAT TCG TTGT-3′ (Reverse); EGFR, 5′-GTG AAA AAC CCC ACC GTTC-3′ (Forward) and 5′- TCT GAA GGG GAG CAA CCT TA-3′ (Reverse). Specific primers for mouse were as follows: DKK1, 5′- TCC CAG AAG AAC CAC ACT GAC TTC-3′ (Forward) and 5′- TCT TGG ACC AGA AGT CTC TTG CAC-3′ (Reverse); GAPDH, 5′- ACC CAG AAG ACT GTG GAT GG-3′ (Forward) and 5′- CAC ATT GGG GGT AGG AAC AC-3′ (Reverse).

Protein extraction and Western blot analysis

The total proteins were extracted from cancer cells and mouse tumors using ice-chilled RIPA lysis buffer containing 50 mM tris-HCl (pH 8.0), 150 mM NaCl, 0.5% sodium deoxycholate, 0.1% SDS, 1% NP-40, 5 mM EDTA, 0.25 mM phenylmethylsulphonyl fluoride, and 1% protease inhibitor cocktail. The concentration of protein was measured using a BCA assay kit (Pierce, Rockford, IL). Subsequently, a volume of 25 ~ 50 μg protein was separated by sodium dodecyl sulfate polyacrylamide gel electrophoresis (SDS-PAGE) gel and transferred onto a polyvinylidene difluoride membrane (Millipore, CA, USA). The membranes were blocked for 1 h at room temperature with 5% skimmed milk or 3% bovine serum albumin dissolved in Tris-buffered saline with 0.1% Tween 20 (TBST). For the proteins with obviously different molecular weight, the PVDF membranes were cut horizontally at each molecular weight location and incubated with the corresponding primary antibodies at 4 °C overnight. After washed with TBST, the membranes were incubated with horseradish peroxidase-conjugated secondary antibodies (1:1000) for 1 h at room temperature. The blots were visualized with the enhanced chemiluminescence plus reagents and digitized into film images using a FluorChem E Imager System (Protein Simple, CA, USA). For the proteins that have very close or overlapping in molecular weight, stripping was used to remove the primary and secondary antibodies of the former protein on the membrane, and then incubated the antibody of the next protein. Quantitation of intensity was performed from 8-bit linear TIF images by LabWorks software (Bio-Rad, USA).

Animals and experimental design

C57BL/6 J Nifdc mice (5 weeks old) and BALB/c Nude mice (5 weeks old) was purchased from Beijing Weitong Lihua Animal Co. All animal procedures were performed in accordance with the guidelines of the Institutional Animal Care and Use Committee of Henan University, and the experimental protocols were approved by the Animal Care and Ethics Committee of Henan University (No. HUSOM2021-072). All animals were housed in 12-h light/dark cycles at a temperature of 20° to 24°C and a relative humidity of 50 ± 10%. All animals were allowed 1 week of acclimatization before the experimental procedures.

To determine whether TMZ could promote DKK1 expression, Luciferase labeled GL261 cells (3×10^5/mouse) were injected into the brains of mice. One week later, the mice were randomly divided into TMZ treatment or control groups. TMZ treatment group were intraperitoneally administrated with 25 mg/kg once daily for 2 weeks, and the control group were intraperitoneally administrated with vehicle containing 5% DMSO, 30% PEG300 and 65% ddH_2O. After that, the mice were euthanized by cervical dislocation. The brains of the mice were removed to examine DKK1 expression.

To determine the role of DKK1 in glioma, DKK1 stably overexpressed or vector-transfected GL261-luciferased cells (3×10^5/mouse) were injected into the brains of mice and allowed to grow 3 weeks. Bioluminescence imaging was used to quantify tumor burden every week by an IVIS Lumina Series III (PerkinElmer). To determine the role of DKK1 in the process of TMZ against glioma, luciferase labeled and stably transfected sh-DKK1- or sh-vector- GL261 cells (3×10^5 cells/mouse) were injected into the brains of randomly grouped mice. After 1 week growth, temozolomide (25 mg/kg) or equal vehicle was intraperitoneally administrated into the mice once daily for 2 weeks. Tumor burden was monitored by luciferase imaging every week after implantation.

To evaluate the anti-tumor effect of TMZ in combination with andrographolide, both C57BL/6 J Nifdc mice and BALB/c nude mice were used to establish the orthotopic models of glioma. Luciferase-labeled GL261 cells (3×10^5 cells/mouse) were implanted into the brains of C57BL/6 J Nifdc mice, and luciferase-labeled U87 cells (2×10^5 cells/mouse) were implanted into the brains of BALB/c nude mice. After one week implantation, the mice were treated with vehicle, TMZ (25 mg/kg, i.p, every day), andrographolide (15 mg/kg, i.p, every other day), or the combination of TMZ and andrographolide for 2 weeks. The survival rate was recorded and the tumor burden was monitored by luciferase imaging and magnetic resonance imaging.

Magnetic resonance imaging (MRI)

We employed a Bruker MRI scanner designed for small animal imaging (BioSpec 70/20 USR; Bruker Corporation). After isoflurane anesthesia, the tumor-bearing mice were fixed in the horizontal position and scanned at different stages of tumor growth. The MRI scan showed coronal T2WI. The sequence parameter settings for T2W1 were as follows: Turbo-RARE sequence, repetition time/echo time = 2500 ms/35 ms, FOV = 20N × 20 mm, image sizes = 200 × 200 mm, slice thicknesses=0.5 mm. The craniocaudal diameter (dcc), the anteroposterior diameter (dap) and the largest lateral diameter (dl) were measured by MRI. Diameter-based measurements were computed to calculate the volume (V): V = 1/6 (dcc×dap×dl×π).

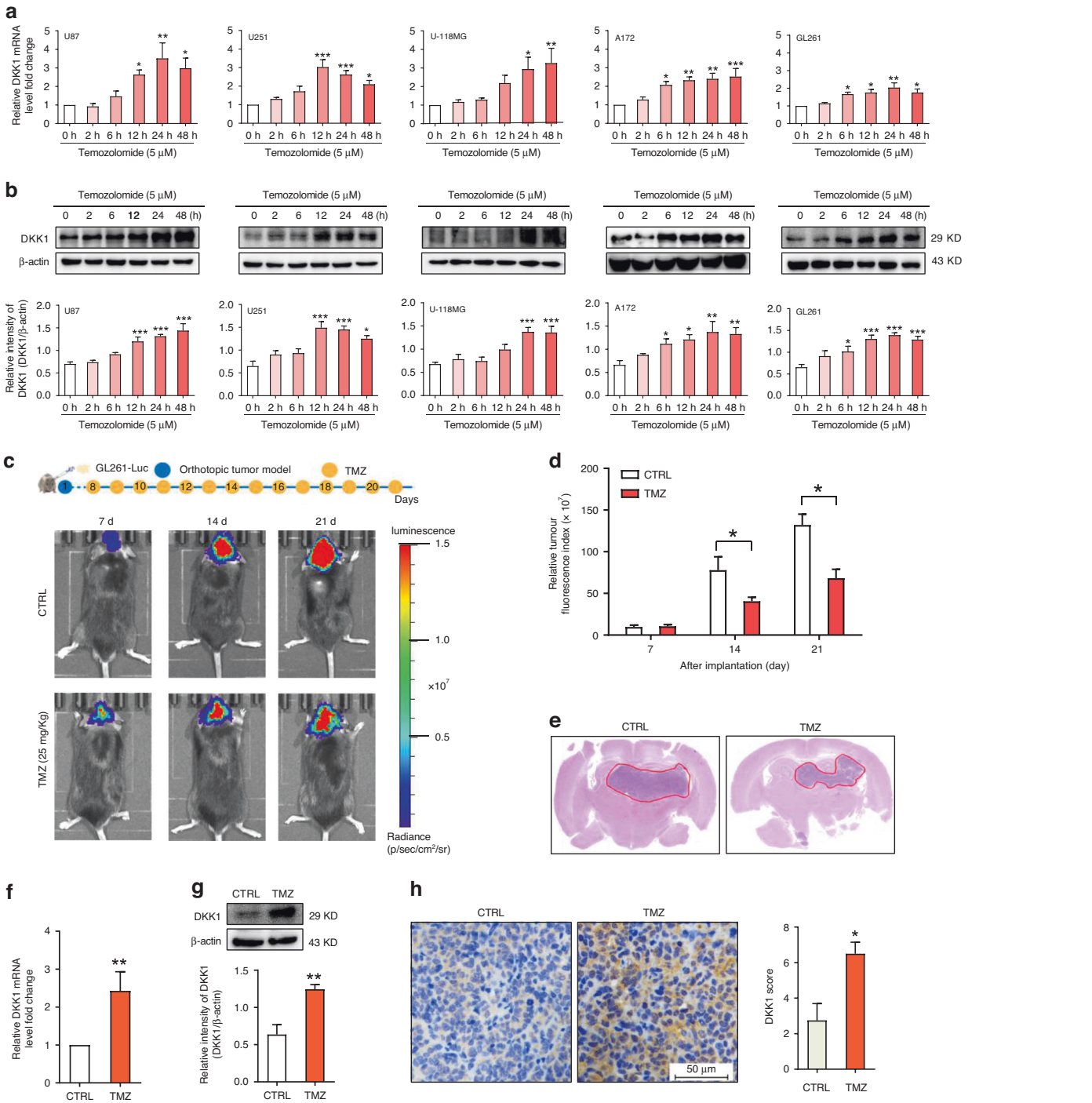

Fig. 1 Temozolomide promotes DKK1 expression in both glioma cells and glioma model of mice. Effects of temozolomide on DKK1 mRNA **a** and protein **b** expression in U87, U251, U-118MG, A172 and GL261 cells. *$p < 0.05$, **$p < 0.01$, ***$p < 0.001$, one-way ANOVA, $n = 6$ independent experiments per group. **c** Representative luminescence images of orthotopic GL261-Luc mouse glioblastoma tumor-bearing C57BL/6 J mice following treatment with vehicle (CTRL) and temozolomide. **d** Quantified luminescence levels using the Lumina IVIS III system. *$p < 0.05$, Two-way ANOVA, $n = 8$ mice per group. **e** H&E staining of whole brain excised on day 21 from GL261-Luc-bearing mice treated with vehicle and temozolomide. Effects of temozolomide on DKK1 mRNA **f** and protein **g** expression in the mice brain tumor tissues from vehicle and TMZ group. **$p < 0.01$, two-tailed unpaired *t*-test, $n = 8$ per group. **h** Immunohistochemical staining of DKK1 in the brain tumor from vehicle and TMZ group. *$p < 0.05$, two-tailed unpaired *t*-test, $n = 8$ per group.

Immunohistochemistry (IHC)

The brains of mice were fixed in 4% paraformaldehyde and embedded in paraffin. Then, the tissue specimens were cut into 4 μm pieces and placed on polylysine-coated slides, followed by xylene deparaffinzation and ethanol gradient rehydration. Histological characteristics were assessed using hematoxylin and eosin (H&E) staining. For IHC staining, the slides were incubated with 3% H_2O_2 for 20 min at room temperature to inactivate the activity of endogenous peroxidase. After boiling in citrate buffer for antigen retrieval and cooling naturally, the slides were incubated overnight at 4 °C with the following antibodies: Rabbit anti-EGFR antibody (1:200), rabbit anti-phospho-AKT (1:100), rabbit anti-phospho-ERK (1:200), rabbit anti-DKK1 (1:200). Subsequently, the slides were incubated with streptavidin-conjugated HRP antibody for 30 min, and developed with diaminobenzidine. Two independent pathologists analyzed the expression

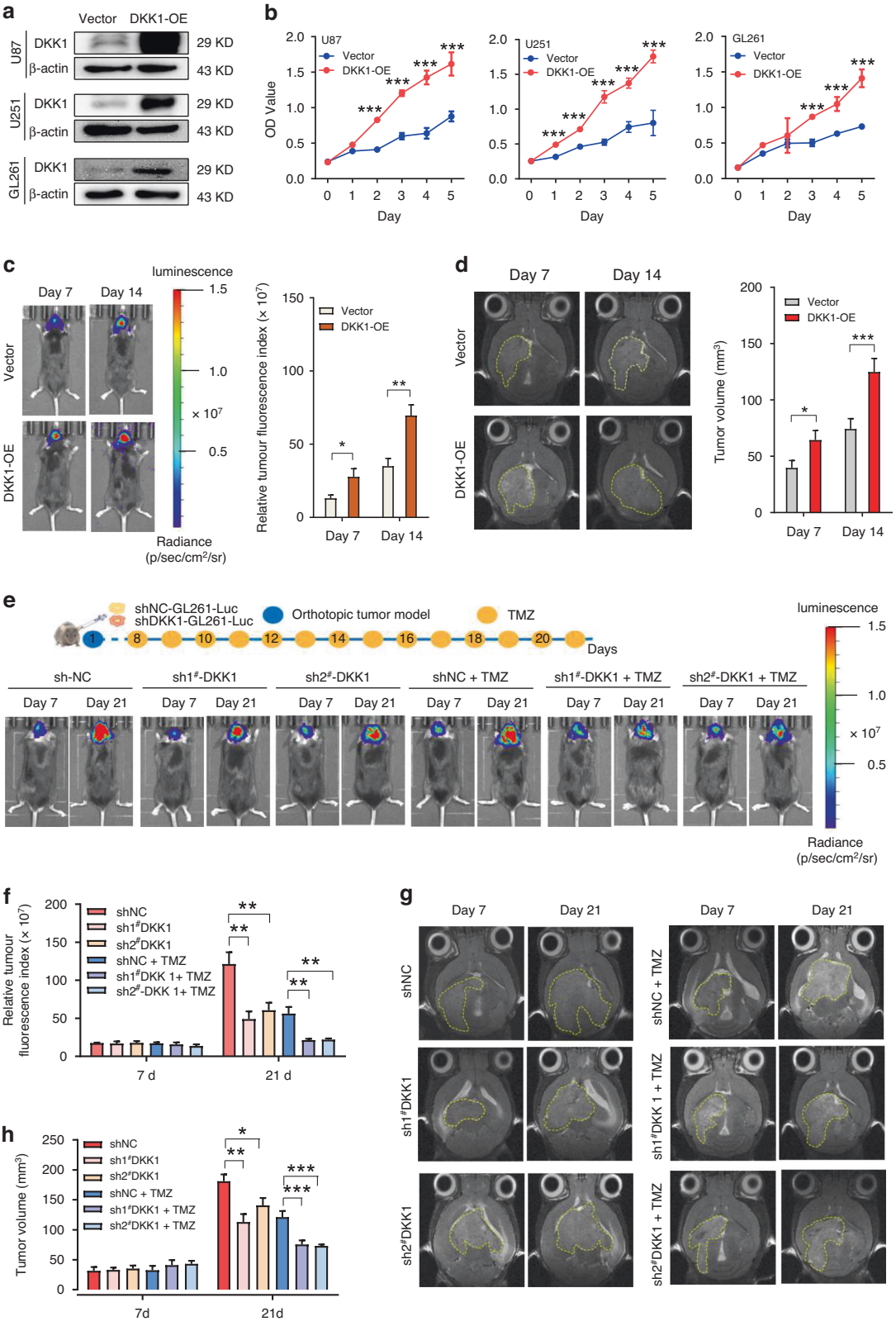

Fig. 2 DKK1 is a sensitizing target for TMZ in glioma. a Western blot analysis of DKK1 expression in U87, U251 and GL261 cells stably transfected with DKK1 plasmid (DKK1-OE) or the empty vector (Vector). **b** Effects of DKK1 overexpression on cell viability in U87, U251 and GL261 glioma cells, ***$p < 0.001$, two-way ANOVA, $n = 6$ independent experiments per group. **c** Quantified luminescence levels of orthotopic GL261-Luc mouse glioblastoma tumor-bearing C57BL/6 J mice collected from vector and DKK1-overexpression (DKK1-OE) groups. *$p < 0.05$, **$p < 0.01$, two-way ANOVA, $n = 10$ mice per group. **d** The volume changes of the tumors from vector and DKK1-overexpression groups were analyzed by 3D MRI. *$p < 0.05$, ***$p < 0.001$, two-way ANOVA, $n = 6$ independent experiments per group. **e** Luminescence images of orthotopic GL261-Luc mouse glioblastoma tumor-bearing C57BL/6 J mice collected from the indicated groups. sh-NC: shRNA vector; TMZ: Temozolomide; sh1$^{\#}$-DKK1: 1$^{\#}$ DKK1 shRNA; sh2$^{\#}$-DKK1: 2$^{\#}$ DKK1 shRNA. **f** Quantified luminescence levels of mice using the Lumina IVIS III System following the indicated treatments. *$p < 0.05$, **$p < 0.01$, two-way ANOVA, $n = 10$ mice per group. **g** Representative MR images of orthotopic GL261-Luc mouse glioblastoma tumor-bearing C57BL/6 J mice collected from the indicated groups. **h** Statistics on the volume changes of the tumors collected from the indicated groups. *$p < 0.05$, **$p < 0.01$, ***$p < 0.001$, two-way ANOVA, $n = 6$ mice per group.

of the target protein in a blinded manner, according to the percentage and intensity of positively stained cells. The percentage of positively stained cells was scored as follows: 0 (negative), 1 (<1%), 2 (2–10%), 3 (11–30%), 4 (31–70%), and 5 (71–100%). The staining intensity was scored as follows: 0 (negative), 1 (weak), 2 (moderate), and 3 (strong). The final IHC score of each tissue was generated by multiplying the percentage score with the staining score.

Brain tissue was detected by HPLC

The mouse brain tissues were rinsed with double steamed water, blotted dry, weighed, and made into 1.0 g/mL homogenate with double steamed water. The homogenate of blank group was taken, and 1 mL methanol solution containing andrographolide reference (1, 2.5, 5, 10, 20, 40 μM) was added, and shaken. After centrifugation (3000 g/min) for 5 min, 1 mL of the supernatant was quantitatively aspirated, dried using a vacuum centrifuge concentrator, and the residue was dissolved with 0.5 mL of methanol shaking, and after centrifugation (12,000 g/min) for 5 min, the supernatant was subjected into UPLC-TQD/MS system. The same procedure was carried out after 1 mL of homogenate from the drug group was taken and 1 mL methanol was added. The analysis was performed using Waters ACQUITY UPLC system (Milford, MA) with a Hypersil GOLD™ column (250 × 4.6 mm, 5 μm particle size; Thermo Scientific). The temperature of the column was set at 30 °C. The samples were separated using acetonitrile (mobile phase A) and water (mobile phase B) at a flow rate of 1 mL/min. The gradient elution programs were as follows: 80–75% B at 0–15 min, 75–72% B at 15–30 min. The injection volume was 10 μL.

Statistical analysis

Statistical analysis was performed using Prism software 7.0 (GraphPad Software Inc., La Jolla, CA, USA). All data were presented as means ± SEM. The significance of the difference between two groups was evaluated using an unpaired Student's *t*-test, while one-way analysis of variance (ANOVA) followed by Dunnett multiple comparison test or 2-way ANOVA followed by Bonferroni post hoc test was used to compare multiple groups. Kaplan-Meier curve and log-rank test were used to evaluate survival between different groups. A value of $p < 0.05$ was considered statistically significant.

RESULTS

Suppression of DKK1 sensitizes glioma cells to temozolomide

To explore whether temozolomide can stimulate DKK1 expression in glioma, we firstly incubated human glioma cell lines U87, U251, A172, U-118MG and mouse glioma cell GL261 with 5 μM temozolomide and examined DKK1 expression. The results showed that temozolomide treatment significantly promoted DKK1 mRNA and protein expression in the glioma cells (Fig. 1a, b). To verify these results in vivo, we established a brain glioma model by injecting luciferase labeled GL261 cells into the brains of C57BL/6 J mice. One week later, the mice were treated with temozolomide (25 mg/kg) or vehicle for 14 consecutive days. Results from bioluminescence images and H&E staining of the brain tissues suggested that TMZ treatment could inhibit tumor progression (Fig. 1c–e). However, real time PCR analysis suggested that TMZ treatment significantly promoted the expression of DKK1 mRNA in the brain tumors (Fig. 1f). Through Western blot and immunohistochemical staining, we also observed an increased expression of DKK1 protein in the brain tumors of TMZ-treated mice (Fig. 1g, h).

To clarify the role of DKK1 in glioma, we established stably DKK1-overexpressed U87, U251 and GL261 cells and examined their proliferation capacity. The construction efficiency was confirmed by western blotting (Fig. 2a). MTT results showed that DKK1-overexpressed cells have a significantly higher proliferation capacity compared to the vector group (Fig. 2b). To confirm these results in vivo, we implanted DKK1-overexpreesed GL261-Luc cells into the brains of C57BL/6 J mice and monitored intracranial tumor growth by bioluminescence imaging. As the results shown that the luciferase activity was significantly increased in the mouse brains of DKK1-overexpressed group (Fig. 2c). Similarly, results from 3D MRI also suggested that the tumor size of DKK1-overexpressed group was larger than that of the vector group (Fig. 2d). Subsequently, we established an orthotopic model of glioma using DKK1-knockdown GL261-Luc cells. One week later, the tumor-bearing mice received 25 mg/kg TMZ once daily for 2 weeks via an intraperitoneal injection. Results from bioluminescence imaging and 3D MRI suggested that knockdown of DKK1 significantly enhances the anti-tumor activity of TMZ in vivo (Fig. 2e–h), indicating that DKK1 is a sensitizing target for TMZ in glioma.

EGFR signaling was involved in temozolomide-induced DKK1 upregulation in glioma

Our previous study has demonstrated that the activation of EGFR promotes DKK1 expression through parallel MEK-ERK and PI3K-Akt signaling pathways in hepatocellular carcinoma [9]. Therefore, we speculated that EGFR signaling was involved in TMZ-mediated the upregulation of DKK1 in glioma. To test our hypothesis, we treated U87, U251, A172, U-118MG and GL261 cells with 5 μM TMZ and examined EGFR expression. Western blot analysis suggested that the protein expression of EGFR level was significantly increased in the glioma cells incubated with temozolomide (Fig. 3a and Supplementary Fig. 1a). Subsequently, we examined the effects of TMZ on PI3K/Akt and MEK/ERK signaling pathways in glioma. As the results shown, TMZ treatment significantly increased the phosphorylation level of Akt and ERK in U87, U251 and GL261 cells (Fig. 3b, c and Supplementary Fig. 1b, c). Consistent with these in vitro results, TMZ treatment also stimulates EGFR, p-AKT and p-ERK protein expression in an orthotopic model of mouse glioma (Fig. 3d).

Furthermore, we reconstituted expression of EGFR in U87, U251 and GL261 cells and examined DKK1 expression. As the results shown, overexpression of EGFR dramatically increased DKK1 mRNA and protein expression in the glioma cells (Fig. 3e, f and Supplementary Fig. 1d, e). Then, we evaluated the effects of the EGFR tyrosine kinase inhibitor AG1478, the Akt inhibitor MK2206, and the MEK inhibitor PD98059 on TMZ-induced expression of DKK1 in glioma cells. Through qRT-PCR assay, we found that pretreated U87, U251 and GL261 cells with these inhibitors for 10 min followed by co-incubation with TMZ for 48 h, the TMZ-induced increase in DKK1 mRNA expression could be dramatically blocked by all the inhibitors (Fig. 3g and

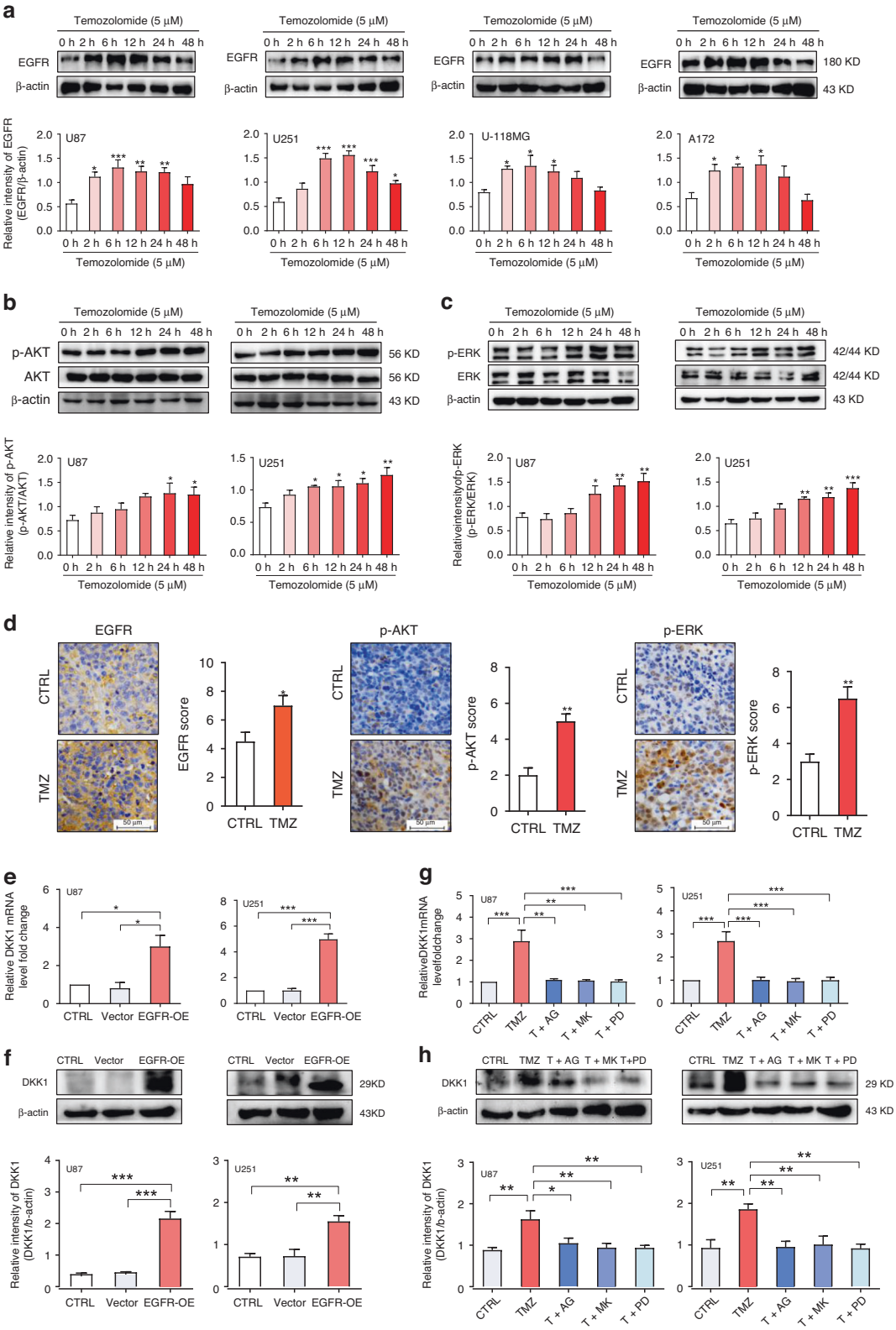

Supplementary Fig. 1f). Similarly, Western blot analysis suggested that all the inhibitors can abrogate TMZ-mediated the up-regulation of DKK1 protein expression in U87, U251 and GL261 cells (Fig. 3h and Supplementary Fig. 1g). Collectively, these results suggested that EGFR signaling participated in TMZ-induced DKK1 expression in glioma.

Andrographolide suppressed DKK1 expression in glioma by inhibiting PI3K/Akt and MEK/ERK signaling pathways

It has been reported that andrographis could inhibit DKK1 expression and enhance the anti-tumor activity of 5-fluorouracil in colorectal cancer [15]. Therefore, we asked whether andrographolide, the major active ingredient of andrographis, could

Fig. 3 EGFR-mediated MEK-ERK and PI3K-Akt pathways are involved in TMZ-induced DKK1 expression in glioma. a Effects of temozolomide on EGFR protein expression in U87, U251, U-118MG, and A172 cells. *$p < 0.05$, **$p < 0.01$, ***$p < 0.001$, one-way ANOVA, $n = 6$ independent experiments per group. Western blot analysis of p-AKT **b** and p-ERK **c** expression in U87 and U251 cells incubated with temozolomide (5 μM). *$p < 0.05$, **$p < 0.01$, ***$p < 0.001$, one-way ANOVA, $n = 6$ independent experiments per group. **d** Immunohistochemical staining of EGFR, p-AKT and p-ERK in the mice brain tumor from vehicle and temozolomide treatment group. *$p < 0.05$, **$p < 0.01$, two-tailed unpaired *t*-test, $n = 8$ per group. Effects of EGFR overexpression on DKK1 mRNA **e** and protein **f** expression in U87 and U251 cells. *$p < 0.05$, **$p < 0.01$, ***$p < 0.001$, one-way ANOVA, $n = 5$ independent experiments per group. Effects of pretreatment with 10 μM AG1478 (an EGFR inhibitor), 5 μM MK2206 (an AKT inhibitor) or 20 μM PD98059 (an MEK inhibitor) on temozolomide-induced DKK1 mRNA **g** and protein **h** expression in U87 and U251 cells. *$p < 0.05$, **$p < 0.01$, ***$p < 0.001$, one-way ANOVA, $n = 5$ independent experiments per group.

suppress DKK1 expression in glioma. As expected, incubated U87, U251 and GL261 cells with 50 μM andrographolide significantly attenuated DKK1 mRNA and protein expression (Fig. 4a–f). Given that the activation EGFR play a critical role in regulating DKK1 expression at transcriptional level, we then assessed the effects of andrographolide on EGFR expression in glioma cells. However, our results revealed that andrographolide could not affect p-EGFR as well as EGFR total protein expression in glioma cells (Fig. 4g–i).

Subsequently, we examined the effects of andrographlide on PI3K/Akt and MEK/ERK signaling pathways in glioma. Through Western blot, we found that andrographlide dramatically reduced the phosphorylation level of Akt and ERK in U87, U251 and GL261 cells (Fig. 5a–c). Meanwhile, the Akt inhibitor MK2206 and MEK inhibitor PD98059 was used to incubate U87, U251 and GL261 cells for 48 h. As shown, both MK2206 and PD98059 suppressed DKK1 mRNA and protein expression in glioma cells (Fig. 5d, e). These results suggested that andrographlide inhibited DKK1 expression through inactivating the MEK-ERK and PI3K-Akt pathways in glioma.

Andrographolide enhances the anti-tumor activity of TMZ by inhibiting DKK1 expression in glioma

To investigate whether andrographolide could inhibit TMZ-mediated the up-regulation of DKK1 expression, we first treated U87 and U251 cells with 50 μM andrographolide for 10 min followed by co-incubation 5 μM TMZ for 48 h. As expected, andrographolide dramatically attenuated DKK1 mRNA and protein expression in glioma cells treated with TMZ (Supplementary Fig. 2a, b).

It has been reported that andrographolide can cross the blood brain barrier and concentrate in the brain [24]. To further confirm it, we first established an orthotopic model of glioma by inoculating GL261-Luc cells into the brains of mice. One week later, andrographolide 15 mg/kg was injected intraperitoneally, and the brain tissue was removed 2 h later, and the presence of andrographolide was detected by HPLC experiments (Supplementary Fig. 3a, b). This result indicated that andrographolide could cross the blood-brain barrier and enter the brain tissue.

Subsequently, we asked whether andrographolide enhanced the efficacy of TMZ against glioma in vivo. Then an orthotopic model of glioma was established. One week later, the tumor-bearing mice were intraperitoneally administrated with andrographolide or/and TMZ for 2 weeks. Results from bioluminescence imaging showed that tumor growth in the andrographolide combined with TMZ group was dramatically decreased compared to single agent treatment and control (Fig. 6a, b). Kaplan-Meier Plotter assay revealed that the combined therapy of TMZ and andrographolide also prolonged mice survival compared to single agent treatment (Fig. 6c).

Furthermore, we established an orthotopic model of glioma by inoculating U87-Luc cells into the brains of BALB/c Nude mice. As expected, results from bioluminescence imaging suggested that andrographolide exhibits the potential to augment the antineoplastic efficacy of TMZ in glioma (Fig. 6d, e). In addition, magnetic resonance images (MRI) were collected on the 7th, 14th and 21st postoperative days, and the results showed that tumor volume in the andrographolide combined with TMZ group was dramatically decreased compared to single agent treatment and control group (Fig. 6f, g). Also, we performed qRT-PCR and Western blotting to examine DKK1 mRNA and protein expression in the brain tumor tissues of the treatment groups and the control group. Consistent with the results of in vitro, andrographolide significantly abrogated TMZ-induced the upregulation of DKK1 mRNA and protein expression in the tumor tissues (Supplementary Fig. 4a, b). IHC analysis further confirmed that andrographolide alleviated TMZ-mediated the up-regulation of DKK1 protein expression (Supplementary Fig. 4c). Taken together, these results indicated that andrographolide can enhance the anti-tumor activity of TMZ against glioma through suppressing DKK1 expression.

DISCUSSION

TMZ is a DNA-alkylating agent, which causes nucleotide mismatch during DNA replication by alkylating the O6 and N7 sites of guanine and N3 position of adenine, thereby exerting its anti-tumor effects [25]. Since the excellent blood-brain barrier (BBB) permeability, TMZ was approved by the US Food and Drug Administration for treating malignant glioma in 2005 [26]. However, large-scale clinical studies have suggested that the clinical benefit of TMZ chemotherapy in glioma patients was very limited, with prolonging the over survival of patients by 2–4 months [27]. Accumulating evidence revealed that hyper-activation of DNA repair pathways, increased efflux of drugs, augmentation of survival autophagy can affect the efficacy of TMZ [28, 29]. In the present study, we first identified that TMZ can promotes DKK1 expression and knockdown of DKK1 sensitizes glioma cells to temozolomide. These findings provide novel insights into TMZ resistance and suggest that DKK1 represents a novel potential target for the treatment of glioma.

DKK1 was originally found to be expressed in the head organizer where it acts as a potent Wnt antagonist to enable the development of the embryonic brain and other organ structures [5, 30]. Given that aberrantly activated Wnt/β-catenin signaling participate in the development and maintenance of glioma, DKK1 was thought to inhibit tumorigenesis of gliomas by blocking the Wnt signaling [31, 32]. Contrast with these reports, our results suggested that overexpression of DKK1 dramatically enhanced tumorigenicity of glioma, indicating that DKK1 functions as a tumor oncogene in glioma. In support of our results, Zhou et al. found that the concentrations of DKK1 in cerebral fluid were significantly higher in glioma patients than in healthy population group or in neuronal benign tumor patients, and the levels of DKK1 protein in tumor tissues were positively correlated glioma grades [33].

DKK1 has been reported to mediate tumor progression by binding to cytoskeleton-associated protein 4 (CKAP4) and subsequent Akt activation [10]. Also, CKAP4 is highly upregulated in glioma and facilitate malignant progression of gliomas via inhibiting Hippo signaling [34]. Therefore, we supposed that DKK1 promotes tumor growth through interacting with CKAP4 in glioma. In addition, because DKK1 can decrease $CD8^+$ tumor-infiltrating lymphocytes and promotes the evasion of NK cell-mediated

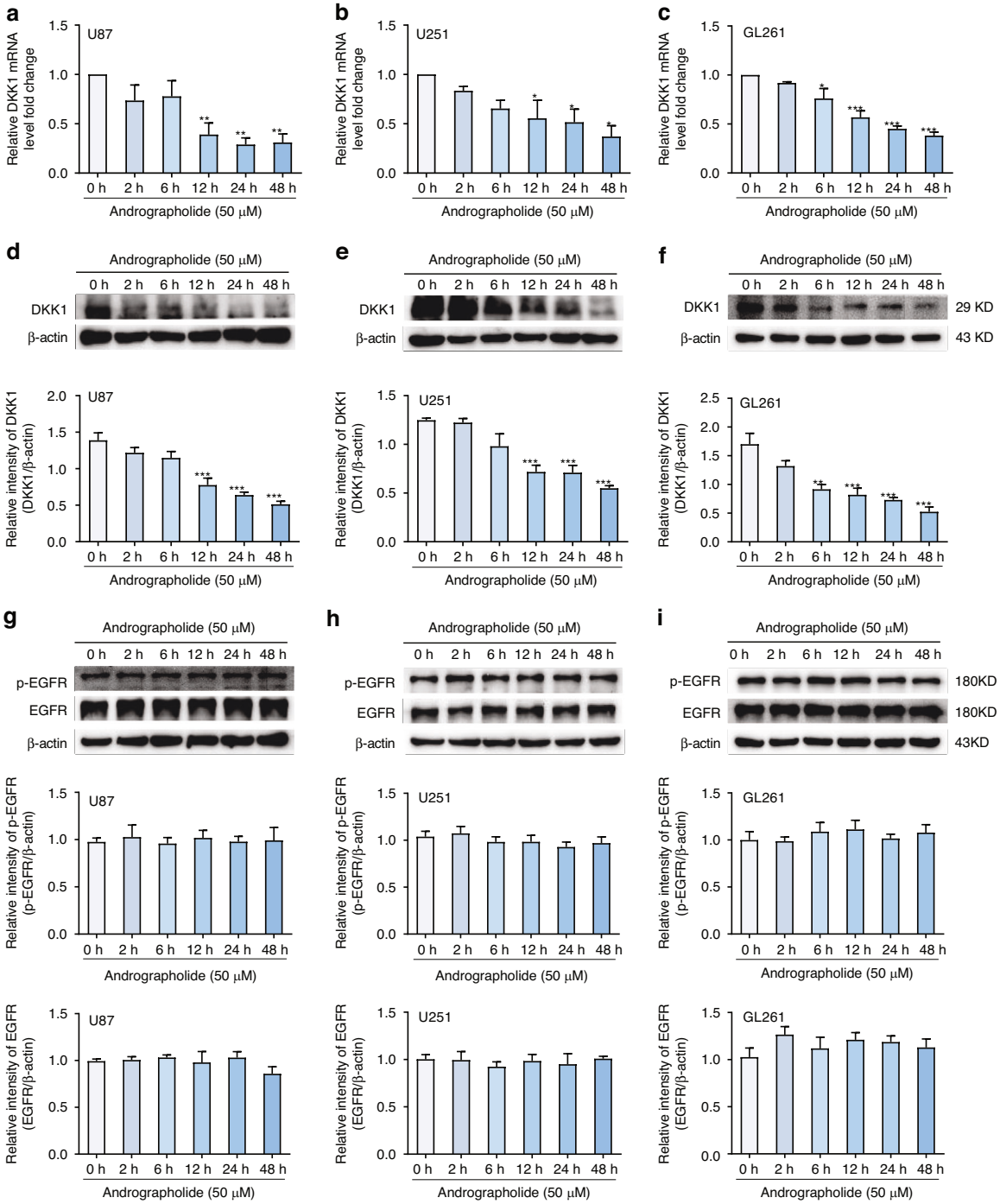

Fig. 4 Andrographolide inhibits DKK1 expression but has no effects on EGFR expression in glioma cells. Real time PCR analysis of DKK1 mRNA expression in U87 **a** U251 **b** and GL261 **c** cells treated with andrographolide. *$p < 0.05$, **$p < 0.01$, ***$p < 0.001$, one-way ANOVA, $n = 5$ independent experiments per group. Western blot analysis of DKK1 protein expression in U87 **d** U251 **e** and GL261 **f** cells incubated with andrographolide. **$p < 0.01$, ***$p < 0.001$, one-way ANOVA, $n = 5$ independent experiments per group. Western blot analysis of p-EGFR and EGFR protein expression in U87 **g** U251 **h** and GL261 **i** cells incubated with andrographolide. one-way ANOVA, $n = 5$ independent experiments per group.

clearance [35], it raises the possibility that DKK1 contributes to tumor progression through suppressing T cell responses in glioma. Of course, the hypothesis needs to be demonstrated in our further study.

EGFR is a transmembrane tyrosine kinase receptor, whose amplification is frequently observed in the lung, breast, colorectal, and liver cancers [36, 37]. EGFR exerting its tumor-promoting effects through the activation of PI3K/Akt, MEK/ERK, and JAK2/STAT signaling pathways [38]. In glioma, EGFR amplification is not only an important biomarker but also contributes to tumorigenesis and progression [39, 40]. Not only that, our study suggested that EGFR amplification and its downstream PI3K/Akt, MEK/ERK signaling pathways contributed to TMZ-induced DKK1 expression in glioma, resulting in a decreased anti-tumor activity of TMZ. In support of our results, studies from several laboratories also found that TMZ treatment could induce EGFR expression in glioma

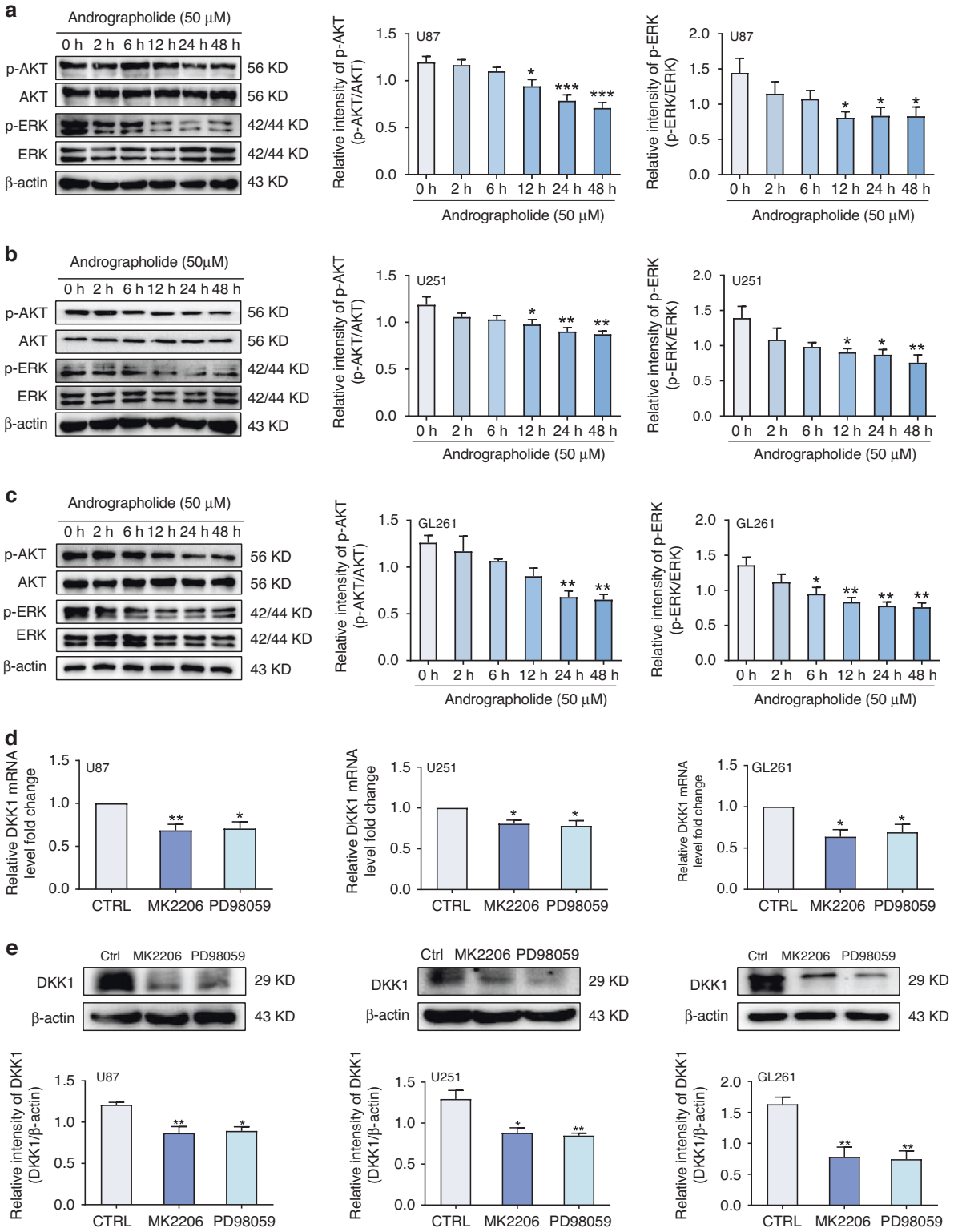

Fig. 5 Andrographolide alleviates DKK1 expression through inhibiting MEK-ERK and PI3K-Akt pathways in glioma cells. Western blot analysis of p-AKT, AKT, p-ERK and ERK protein expression in U87 **a**, U251 **b** and GL261 **c** cells incubated with andrographolide. *$p < 0.05$, **$p < 0.01$, ***$p < 0.001$, one-way ANOVA, $n = 5$ independent experiments per group. Effects of 5 μM MK2206 (an AKT inhibitor) and 20 μM PD98059 (an ERK inhibitor) on DKK1 mRNA **d** and protein **e** expression in U87, U251 and GL261 cells. *$p < 0.05$, **$p < 0.01$, one-way ANOVA, $n = 5$ independent experiments per group.

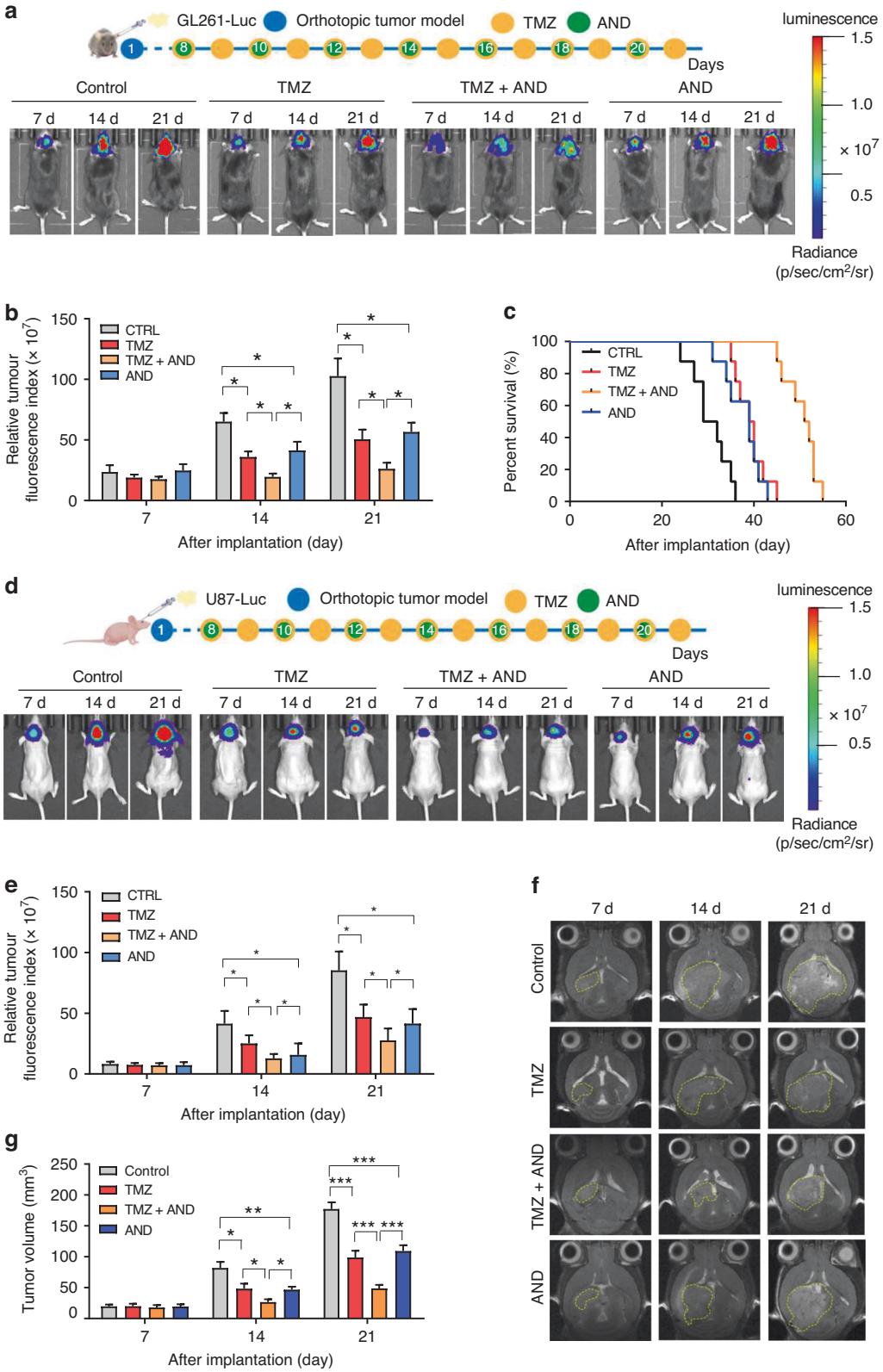

[41, 42]. Unfortunately, it was reported that the combination of small-molecule tyrosine kinase inhibitors (TKIs) with TMZ has not achieved therapeutic benefit in the treatment of glioma [43]. The possibility is that compensatory activation of other RTKs and an intact blood-brain barrier contributes to anti-EGFR therapy failure. Based on the reasons, several strategies targeting EGFR have been developed to enhance the TMZ therapy effects. For example, Meng et al. developed a nanoinhibitor, BIP-MPC-NP, which can easily cross the BBB and restrain temozolomide-resistant glioma by attenuating EGFR and MET signaling [44]. Danhier et al.

Fig. 6 Andrographolide enhances the antitumor effect of temozolomide by inhibiting DKK1 in an orthotopic model of glioma. **a** Representative luminescence images of orthotopic GL261-Luc mouse glioblastoma tumor-bearing C57BL/6 J mice following treatment with vehicle (CTRL), temozolomide (TMZ), temozolomide combined with andrographolide (TMZ + AND), and andrographolide (AND). **b** Quantified luminescence levels of mice using the Lumina IVIS III System following the indicated treatments. *$p < 0.05$, two-way ANOVA, $n = 8$ mice per group. **c** Kaplan-Meier survival curve of mice in indicated groups. **d** Representative luminescence images of orthotopic U87-Luc mouse glioblastoma tumor-bearing BALB/c Nude mice following treatment with vehicle (CTRL), temozolomide (TMZ), temozolomide combined with andrographolide (TMZ + AND), and andrographolide (AND). **e** Quantified luminescence levels of mice using the Lumina IVIS III System following the indicated treatments. *$p < 0.05$, two-way ANOVA, $n = 8$ mice per group. **f** Representative MR images of mouse head from vehicle (CTRL), temozolomide (TMZ), temozolomide combined with andrographolide (TMZ + AND), and andrographolide (AND) groups at selected times. **g** Statistics on the volume changes of the tumors collected from the indicated groups at different time points. *$p < 0.05$, **$p < 0.01$, ***$p < 0.001$, two-way ANOVA, $n = 6$ mice per group.

demonstrated that the combination of anti-Galectin-1 and anti-EGFR siRNA-loaded chitosan-lipid nanocapsules decrease temozolomide resistance in glioblastoma [45]. Collectively, these studies provide insights into developing new strategies capable of potentially overcoming TMZ-resistance for the treatment of glioma patients.

Over the past years, several studies have shown that andrographolide could inhibit the proliferation and migration of human glioblastoma cells in vitro [20, 23]. Since andrographolide can cross the blood brain barrier and concentrate in the brain [24], it raises the possibility that andrographolide can be used as a potential chemotherapy drug for the treatment of glioma. Indeed, our results indicated that andrographlide could suppress TMZ-induced DKK1 overexpression accompanied with the enhanced anti-tumor effects in glioma. As mentioned above, TMZ promotes DKK1 expression through the EGFR signaling in glioma. However, our findings suggested that andrographlide did not affect EGFR expression but inhibited the downstream MEK/ERK and PI3K/Akt signaling pathways, leading to decreased DKK1 expression. In line with our results, Li et al. found that andrographolide inhibits the proliferation of human glioblastoma cells by reducing the activity of PI3K/Akt signaling [20].

Notably, multiphoton intravital imaging has achieved great progress in detecting some compounds crossing the intact blood-brain barrier [46]. However, we cannot detect andrographolide distribution in the brain tissue by fluorescence imaging owing to the lack of fluorescent groups in andrographolide. Although we observed that andrographolide can be detected by HPLC in the brain tissue of tumor-bearing mice after 2 h injection intraperitoneally, current data do not allow determination of whether andrographolide is in the cerebral vasculature or crosses the blood-brain barrier into the brain parenchyma, this is a limitation of our study.

In conclusion, TMZ promotes DKK1 expression at the transcriptional level through the activation of EGFR and its downstream MEK-ERK and PI3K-Akt signaling, conferring glioma cell resistance to TMZ; inhibition of DKK1 expression by andrographolide dramatically increases the sensitivity to TMZ treatment in murine glioma models. Our study provides the first evidence that andrographolide may be used as a potential adjunct to routine chemotherapy for glioma.

DATA AVAILABILITY

The datasets used and/or analyzed during the current study are available from the corresponding author on reasonable request.

REFERENCES

1. Kannan S, Murugan AK, Balasubramanian S, Munirajan AK, Alzahrani AS. Gliomas: genetic alterations, mechanisms of metastasis, recurrence, drug resistance, and recent trends in molecular therapeutic options. Biochem Pharm. 2022;201:115090.
2. Venkataramani V, Schneider M, Giordano FA, Kuner T, Wick W, Herrlinger U, et al. Disconnecting multicellular networks in brain tumours. Nat Rev Cancer. 2022;22:481–91.
3. Tong S, Wang Y, Wu J, Long J, Zhong P, Wang B. Comprehensive pharmacogenomics characterization of temozolomide response in gliomas. Eur J Pharm. 2021;912:174580.
4. Lang F, Liu Y, Chou FJ, Yang C. Genotoxic therapy and resistance mechanism in gliomas. Pharm Ther. 2021;228:107922.
5. Glinka A, Wu W, Delius H, Monaghan AP, Blumenstock C, Niehrs C. Dickkopf-1 is a member of a new family of secreted proteins and functions in head induction. Nature. 1998;391:357–62.
6. Jumpertz S, Hennes T, Asare Y, Schutz AK, Bernhagen J. CSN5/JAB1 suppresses the WNT inhibitor DKK1 in colorectal cancer cells. Cell Signal. 2017;34:38–46.
7. Kim HY, Park JH, Won HY, Lee JY, Kong G. CBX7 inhibits breast tumorigenicity through DKK-1-mediated suppression of the Wnt/beta-catenin pathway. FASEB J. 2015;29:300–13.
8. Zhang H, Yu C, Dai J, Keller JM, Hua A, Sottnik JL, et al. Parathyroid hormone-related protein inhibits DKK1 expression through c-Jun-mediated inhibition of beta-catenin activation of the DKK1 promoter in prostate cancer. Oncogene. 2014;33:2464–77.
9. Niu J, Li W, Liang C, Wang X, Yao X, Yang RH, et al. EGF promotes DKK1 transcription in hepatocellular carcinoma by enhancing the phosphorylation and acetylation of histone H3. Sci Signal. 2020;13:eabb5727.
10. Kimura H, Sada R, Takada N, Harada A, Doki Y, Eguchi H, et al. The Dickkopf1 and FOXM1 positive feedback loop promotes tumor growth in pancreatic and esophageal cancers. Oncogene. 2021;40:4486–502.
11. Shen Q, Fan J, Yang XR, Tan Y, Zhao W, Xu Y, et al. Serum DKK1 as a protein biomarker for the diagnosis of hepatocellular carcinoma: a large-scale, multicentre study. Lancet Oncol. 2012;13:817–26.
12. Chu HY, Chen Z, Wang L, Zhang ZK, Tan X, Liu S, et al. Dickkopf-1: a promising target for cancer immunotherapy. Front Immunol. 2021;12:658097.
13. Kikuchi A, Matsumoto S, Sada R. Dickkopf signaling, beyond Wnt-mediated biology. Semin Cell Dev Biol. 2022;125:55–65.
14. Salim H, Zong D, Haag P, Novak M, Mork B, Lewensohn R, et al. DKK1 is a potential novel mediator of cisplatin-refractoriness in non-small cell lung cancer cell lines. BMC Cancer. 2015;15:628.
15. Zhao Y, Wang C, Goel A. Andrographis overcomes 5-fluorouracil-associated chemoresistance through inhibition of DKK1 in colorectal cancer. Carcinogenesis. 2021;42:814–25.
16. Agbarya A, Ruimi N, Epelbaum R, Ben-Arye E, Mahajna J. Natural products as potential cancer therapy enhancers: a preclinical update. SAGE Open Med. 2014;2:2050312114546924.
17. Ouyang L, Luo Y, Tian M, Zhang SY, Lu R, Wang JH, et al. Plant natural products: from traditional compounds to new emerging drugs in cancer therapy. Cell Prolif. 2014;47:506–15.
18. Zhang H, Li S, Si Y, Xu H. Andrographolide and its derivatives: current achievements and future perspectives. Eur J Med Chem. 2021;224:113710.
19. Malik Z, Parveen R, Parveen B, Zahiruddin S, Aasif Khan M, Khan A, et al. Anticancer potential of andrographolide from Andrographis paniculata (Burm.f.) Nees and its mechanisms of action. J Ethnopharmacol. 2021;272:113936.
20. Li Y, Zhang P, Qiu F, Chen L, Miao C, Li J, et al. Inactivation of PI3K/Akt signaling mediates proliferation inhibition and G2/M phase arrest induced by andrographolide in human glioblastoma cells. Life Sci. 2012;90:962–7.
21. Zhang J, Li C, Zhang L, Heng Y, Wang S, Pan Y, et al. Andrographolide, a diterpene lactone from the Traditional Chinese Medicine Andrographis paniculate, induces senescence in human lung adenocarcinoma via p53/p21 and Skp2/p27. Phytomedicine. 2022;98:153933.
22. Bodiga VL, Bathula J, Kudle MR, Vemuri PK, Bodiga S. Andrographolide suppresses cisplatin-induced endothelial hyperpermeability through activation of PI3K/Akt and eNOS -derived nitric oxide. Bioorg Med Chem. 2020;28:115809.
23. Yang SH, Wang SM, Syu JP, Chen Y, Wang SD, Peng YS, et al. Andrographolide induces apoptosis of C6 glioma cells via the ERK-p53-caspase 7-PARP pathway. Biomed Res Int. 2014;2014:312847.

24. Lu J, Ma Y, Wu J, Huang H, Wang X, Chen Z, et al. A review for the neuroprotective effects of andrographolide in the central nervous system. Biomed Pharmacother. 2019;117:109078.
25. Ortiz R, Perazzoli G, Cabeza L, Jimenez-Luna C, Luque R, Prados J, et al. Temozolomide: an updated overview of resistance mechanisms, nanotechnology advances and clinical applications. Curr Neuropharmacol. 2021;19:513–37.
26. Desai R, Suryadevara CM, Batich KA, Farber SH, Sanchez-Perez L, Sampson JH. Emerging immunotherapies for glioblastoma. Expert Opin Emerg Drugs. 2016;21:133–45.
27. Cruz JVR, Batista C, Afonso BH, Alexandre-Moreira MS, Dubois LG, Pontes B, et al. Obstacles to glioblastoma treatment two decades after temozolomide. Cancers. 2022;14:3203.
28. Vilar JB, Christmann M, Tomicic MT. Alterations in molecular profiles affecting glioblastoma resistance to radiochemotherapy: where does the good go? Cancers. 2022;14:2416.
29. Tomar MS, Kumar A, Srivastava C, Shrivastava A. Elucidating the mechanisms of Temozolomide resistance in gliomas and the strategies to overcome the resistance. Biochim Biophys Acta Rev Cancer. 2021;1876:188616.
30. Grotewold L, Theil T, Ruther U. Expression pattern of Dkk-1 during mouse limb development. Mech Dev. 1999;89:151–3.
31. Reis M, Czupalla CJ, Ziegler N, Devraj K, Zinke J, Seidel S, et al. Endothelial Wnt/beta-catenin signaling inhibits glioma angiogenesis and normalizes tumor blood vessels by inducing PDGF-B expression. J Exp Med. 2012;209:1611–27.
32. Kahlert UD, Maciaczyk D, Doostkam S, Orr BA, Simons B, Bogiel T, et al. Activation of canonical WNT/beta-catenin signaling enhances in vitro motility of glioblastoma cells by activation of ZEB1 and other activators of epithelial-to-mesenchymal transition. Cancer Lett. 2012;325:42–53.
33. Zhou Y, Liu F, Xu Q, Wang X. Analysis of the expression profile of Dickkopf-1 gene in human glioma and the association with tumor malignancy. J Exp Clin Cancer Res. 2010;29:138.
34. Luo T, Ding K, Ji J, Zhang X, Yang X, Chen A, et al. Cytoskeleton-associated protein 4 (CKAP4) promotes malignant progression of human gliomas through inhibition of the Hippo signaling pathway. J Neurooncol. 2021;154:275–83.
35. Sui Q, Liu D, Jiang W, Tang J, Kong L, Han K, et al. Dickkopf 1 impairs the tumor response to PD-1 blockade by inactivating CD8+ T cells in deficient mismatch repair colorectal cancer. J Immunother Cancer. 2021;9:e001498.
36. Sigismund S, Avanzato D, Lanzetti L. Emerging functions of the EGFR in cancer. Mol Oncol. 2018;12:3–20.
37. Woodburn JR. The epidermal growth factor receptor and its inhibition in cancer therapy. Pharm Ther. 1999;82:241–50.
38. Wee P, Wang Z. Epidermal growth factor receptor cell proliferation signaling pathways. Cancers. 2017;9:52.
39. Oprita A, Baloi SC, Staicu GA, Alexandru O, Tache DE, Danoiu S, et al. Updated insights on EGFR signaling pathways in glioma. Int J Mol Sci. 2021;22:587.
40. Huang PH, Xu AM, White FM. Oncogenic EGFR signaling networks in glioma. Sci Signal. 2009;2:re6.
41. Munoz JL, Rodriguez-Cruz V, Greco SJ, Ramkissoon SH, Ligon KL, Rameshwar P. Temozolomide resistance in glioblastoma cells occurs partly through epidermal growth factor receptor-mediated induction of connexin 43. Cell Death Dis. 2014;5:e1145.
42. Wang Z, Hu P, Tang F, Lian H, Chen X, Zhang Y, et al. HDAC6 promotes cell proliferation and confers resistance to temozolomide in glioblastoma. Cancer Lett. 2016;379:134–42.
43. Artene SA, Tuta C, Dragoi A, Alexandru O, Stefana Oana P, Tache DE, et al. Current and emerging EGFR therapies for glioblastoma. J Immunoass Immunochem. 2018;39:1–11.
44. Meng X, Zhao Y, Han B, Zha C, Zhang Y, Li Z, et al. Dual functionalized brain-targeting nanoinhibitors restrain temozolomide-resistant glioma via attenuating EGFR and MET signaling pathways. Nat Commun. 2020;11:594.
45. Danhier F, Messaoudi K, Lemaire L, Benoit JP, Lagarce F. Combined anti-Galectin-1 and anti-EGFR siRNA-loaded chitosan-lipid nanocapsules decrease temozolomide resistance in glioblastoma: in vivo evaluation. Int J Pharm. 2015;481:154–61.
46. Qin RX, Li S, Qiu YW, Feng YS, Liu YQ, Ding DD, et al. Carbonized paramagnetic complexes of Mn (II) as contrast agents for precise magnetic resonance imaging of sub-millimeter-sized orthotopic tumors. Nat Commun. 2022;13:1938.

ACKNOWLEDGEMENTS

This study was supported by the National Key R&D Program of China (2021YFA0909600), Natural Science Foundation of Henan (232300420050), Key projects of Henan Science and Technology Department (232102311115, 242102311032, 242102311072). This work was also supported by the Open Projects in the Key Laboratory for Neuroscience of Peking University.

AUTHOR CONTRIBUTIONS

ZSZ, ZXG, JJH, CM, HTT, FYZ, YNC, CQX, JQL, and ZZL carried out the experiments, LLH and HS performed the data analysis, SQX and DF designed this study and wrote the manuscript.

COMPETING INTERESTS

The authors declare no competing interests.

CONSENT TO PUBLISH

All contributing authors agree to the publication of this article.

ADDITIONAL INFORMATION

Supplementary information The online version contains supplementary material available at https://doi.org/10.1038/s41416-024-02842-0.

Correspondence and requests for materials should be addressed to Hua Sun, Song-Qiang Xie or Dong Fang.